International Journal of Computer Information Systems and Industrial Management Applications
ISSN 2150-7988 Volume 18(3s) 2026 pp. 1272-1291
https://doi.org/10.70917/ijcisim-2026-2460
Article

A Meta-Learner Driven CNN–Transformer Stacked Ensemble for High-Accuracy Brain Tumor Classification

Namrata Vijayvargiya[1], Nirupma Singh[2]

[1]Research Scholar, School of Engineering & Technology,Career Point University, Kota, Rajasthan, India
[2]Assistant Professor, School of Engineering & Technology, Career Point University, Kota, Rajasthan, India
namratavj528@gmail.com , nirupmasingh1511@gmail.com

Abstract: Diagnosis of brain tumor with Magnetic Resonance Imaging (MRI) is the key for early treatment planning, which however, manual interpretation of can be time-consuming and may suffer from diagnostic inconsistency. To overcome this issue, in this paper, a stacked ensemble-based hybrid deep learning framework for multi-class brain tumor classification is proposed. The combination consists of Xception, ConvNeXt and Swin Transformer as heterogeneous base learners, their probabilistic predictions are combined by the meta-learner via stacking. Large data preprocessing and augmentation improve generalization and robustness. Experimental results on a balanced MRI task achieve a test accuracy of 98.92%, as well as high precision, recall and F1-scores for all tumor classes are obtained. The confusion matrix and the ROC analyses demonstrated a high-performance discrimination power and low misclassification. The proposed method yields a practical and scalable solution for automated MRI-based brain tumor diagnosis, laying the foundation for future clinical decision-support systems.
Keywords: Brain Tumor Classification, MRI, Stacked Ensemble, CNN–Transformer, Meta-Learning, Deep Learning, Medical Image Analysis

1. Introduction

Brain tumors are one of the deadliest neurologic diseases in which early and accurate diagnosis greatly impacts treatment strategy as well as patient's survival. Magnetic Resonance Imaging (MRI) constitutes the ideal imaging modality because of its high soft tissue contrast and absence of ionizing radiation and for obtaining structural information at high resolution [1]. However, manual MRI analysis is time-consuming and subjective, as well as significantly dependent on radiological expertise. Differences in tumor size, shape, intensity and location also add to the difficulty of diagnosis. As a result, computer–aided diagnosis systems are becoming more important in neuro-oncology and such systems based on artificial intelligence have emerged [2].

Recent developments in deep learning techniques such as Convolutional Neural Networks (CNNs) and Transformer-based architecture exhibit high capability in the detection or classification of tumors. Convolutional Neural Networks (CNNs) are good at encoding local texture and spatial information [3], while Transformers possess strong ability of modeling long-range dependencies and global context information. However, single-model methods usually suffer from correlated errors and lack of generalization on small medical datasets, as well as sensitivity to data imbalance. Such challenges have motivated the investigation and synthesis of hybrid ensemble approaches that combine various architectures to improve robustness and reliability [4].

In this work the focus is on multi-class brain tumor classification of MRI images, and we aim to design a novel stacked ensemble hybrid deep learning model [5]. The proposed structure integrates three base learners with different architectures, including Xception, ConvNeXt and Swin Transformer, to exploit the complementary local features. The outputs are stacked using a meta-learner, and this fusion strategy allows its decision to be adaptive and data dependent. This architecture was specifically developed to minimize the occurrence of correlated errors, enhance that of generalization and further ensure clinically sound classifier performance.

The main novelty of this work is:

- Unifying CNN-based and Transformer-based architectures under a single stacking framework.
- Utilizing architectural diversity to learn the fine sweaty texture, hierarchical features and global context together.
- Improving the stability of probabilistic fusion by using a meta-learning approach.
- Exceeding state-of-the-art performance with a balanced class-wise accuracy and very low overfitting.

The organization of the remainder of this paper is as follows: Section 2 briefly introduce related works of deep learning-based brain tumor classification and segmentation. The proposed stacked ensemble method is introduced in Section 3. Implementation details, dataset description and experimental settings are described in Section 4. Section 5 presents quantitative and qualitative results, such as accuracy, loss behavior and confusion matrix performance measures. Finally, Section 6 presents conclusion and future work.

2. Literature review

Tumors of the brain are one of the most severe neurological diseases, with their prognosis being dependent on early-stage detection that can aid in improving treatment decisions. Magnetic Resonance Imaging (MRI) is extensively used in comparison to other imaging techniques owing to excellent soft tissue contrast and multi-structural information without ionizing radiation. Recent systematic reviews according to PRISMA guidelines find that deep learning algorithms, in particular hybrid CNN–Transformer models, significantly outperform traditional methods and surpass Dice scores of 90% on benchmark datasets [1]. As imaging volumes and diagnostic challenges continue to grow, artificial intelligence (AI) systems have become necessary support tools for radiologists. Novel architecture such as transfers learning, attention mechanisms, autoencoders and transformers have paved the way to diagnosis errors reduction and classification/segmentation improvement; however, limitations with respect to interpretability and dataset bias persist [2].

The field of brain tumor segmentation has evolved rapidly with the use of deep learning techniques and multimodal MRI. Architectures like CNNs, U-Net variants and combination with attention are showing enhanced tumour-localization ability and generalization on benchmark datasets such as BraTS or TCGA-GBM [3]. Bibliometric analysis of hundreds of papers shows that research activity has experienced a dramatic increase, with CNN based deep and the hybrid architecture becoming more predominant in current contributions, as the multi-disciplinary nature of this area expands [4]. Scientometric analysis also indicates the growing application of deep learning in MRI-based tumor classification studies and recognizes new research directions and international collaborations that influence future development of neuro-oncology AI systems [5].

Recent comparative studies, that systematically compared CNN, transformers and hybrid architectures, potential benefits of hybrid models to be superior reaching Dice scores higher than 0.90, and classification accuracy greater than 98% to multiple MRI datasets [6]. The Brain Tumor Segmentation (BraTS) challenges have been forefront in facilitating this advancement by making available publicly standardized datasets, advanced annotations, and benchmarking protocols which have significantly increased the state-of-art segmentation results [7]=[10]. In glioma segmentation, moving from 2D-CNN-based methods to 3D ones and the recent introduction of attention mechanisms, transformers, and ensemble learning have greatly boosted tumor delineation as well as survival prediction - demonstrating the importance of explainable and multimodal AI systems [8].

The hybrid detection–segmentation-based pipelines have also shown strong clinical relevance. For instance, cascaded models such as YOLO-detector-on-U-Net-segmentation produce larger Dice and mAP scores in relation to single-stage classifiers, allowing for more accurate tumor localization [9]. Pretrained CNN models following a transfer learning strategy demonstrate the strength of deep learning in tumor classification, which frequently obtains an accuracy rate later 98% for large MRI dataset [10]. Salient architectures such as those built upon DenseNet as well and empowered by explainable AI technique like Grad-CAM++ bring high accuracy and interpretable tumor localization, which promotes clinical dependability [11].

Recent comprehensive reviews on deep learning applications in neuro-oncology emphasize the efficacy of contemporary architecture and reveal persisting challenges such as inconsistent benchmarking, lack of diversity for the dataset used in deep learning training or clinical deployment due to regulatory limitations [12]. Systematical research over hundreds of segmentation models indicates that CNN, GAN, U-Net and hybrid architecture all improve accuracy and interpretability greatly, but the real application still encounters problems of data imbalance and hyperparameter sensitivity [13]. Ensemble methods and integrated frameworks such as VISION integrate

classification, detection and segmentation into one pipeline structure and perform well in multiple orientations of MRI with improved clinical efficiency [14].

Comparative analyses of state-of-the-art CNN architectures (VGG, ResNet, Inception and EfficientNets) demonstrate that advanced networks, like EfficientNetV2 provide better performance in binary as well as multiclass tumor classification tasks [15]. The studies demonstrated that the CNN-based and hybrid CNN–Transformer models outperform conventional approaches, leading to accurate tumor delineation with multimodal data fusion [16]. Hybrid machine learning and deep learning techniques have improved diagnostic accuracy in datasets such as BraTS and TCIA, facilitating personalized treatments for neuro-oncology [17].

Another necessary alternative of the neural network can be either ensemble or hybrid model for its more reliable performance. Multi-model approaches, such as InceptionV3–Xception ensembles are reported to surpass 98% of classification accuracy, showing the applications of ensemble methods [18]. Attention based architectures such as the OA-U-Net-PVT are the approaches that have been proposed to fuse the transformers along with U-Net to enhance spatial and contextual understanding and reaches high accuracy in terms of Dice score [19]. Similar advances are made in multimodal MRI-based glioma segmentation, where the application of attention- and transformer-based models enhances treatment planning although data quality and interpretability remain an issue [20].

Ensemble U-Net models have also widely shown high performance in detection, segmentation, or classification tasks of the deep learning system that get higher Dice scores and more clinical robustness over BraTS datasets [21]. The release of large-scale datasets with diverse scenarios, e.g., BTS-DS 2024, has further proposed progress for research and made the state-of-the-art detection and segmentation performance can be achieved by modern YOLO-based models [22]. Rreviews based onAI-driven diagnostic systems have underscored the increasing importance of CNN, GAN and transformers and ensemble methods, focusing on accuracy improvements despite challenges in applicability to other patient populations and integration into clinical workflows [23].

Diverse and fair data have drawn research attention more than ever. Experiments on the BraTS-Africa data show that augmentation and ensemble can benefit class imbalance for a fair clinical evaluation [24]. Hybrid computational flow mixing classical and deep-learning-based machine learning algorithms, such as ICA2-SVM architectures, are still being reported with high accuracy and computation efficiency [25], demonstrating that the ML–DL integration is still actively required. Multi-task learning methods that integrate segmentation and classification promote diagnostic accuracy, yielding competitive Dice and accuracy on different tumor classes [26].

Meanwhile, two-stage YOLO + AT-UNet methods show better performance in terms of precision, recall and Dice under the same protocol [27]. Apart from traditional computer-aided diagnosis, by combining segmentation with interactive 3D visualization, augmented reality solutions such as BrainAR allow for intuitive clinical interpretation and real-time patient-specific analysis [28]. Fuzzy theories and CNNs combined achieve high accuracy for classification and Dice scores, as well as tumor size estimation for clinical decision making [29].

A survey on machine learning-based diagnostic frameworks demonstrates how different preprocessing, segmentation, and classification steps enhance computer-aided diagnosis systems as well as future research directions in the field of neurological disorder detection [30]. As an example, advanced detection-oriented architectures like DC-YOLOv8FEN integrate transformers, attention modules and optimized loss functions to obtain high accuracy and robustness in case of rare tumor detection [31]. Newer segmentation methods integrate topological data analysis in U-Net type architectures, achieving even higher Dice performances by also considering the local and global aspects of tumor shapes [32].

3D Sparse Segmentation Models [33] Faster computation is possible using 3D segmentation models that incorporate densely connected convolutions together with bi-directional ConvLSTM layers as well achieving competitive accuracy in BraTS datasets. In summary, from early CNN-based on brain tumor classification models to attention-based transformers and hybrid CNN–Transformer architectures, we can see that hybrid approaches provide the best trade-off between local feature extraction and global context modeling. Yet limitations such as domain shift, data paucity and explainability still steer the research into federated learning, self-supervised learning and trustworthy AI systems [34].

Recent research also reports on the effectiveness of automatic deep learning tools for detection of brain tumors. Hybrid CNN, attention module with transfer learning-based architectures enhances on generalization and decrease KLC related errors [35]. CNN-XGBoost models, which are intentionally embedded in adaptive approaches and become fine-tunable with breathing-induced motion (BIM) samples, reach an apparent accuracy of 99% and

effectively segment tumor region across different datasets [36]. In imbalanced datasets, attention learning models and comparative CNN works can achieve better classification accuracy and robustness [37], [38]. Newer architectures that introduce multilevel feature extraction, attention mechanisms and transformers achieve superior classification precision and stability beyond 98% [39], [40]. Deep-learning systems based on IoMT also can accomplish real-time diagnosis accuracy > 99%, showing a great prospect for remote and scalable healthcare applications [41].

3. Methodology

3.1 proposed architecture

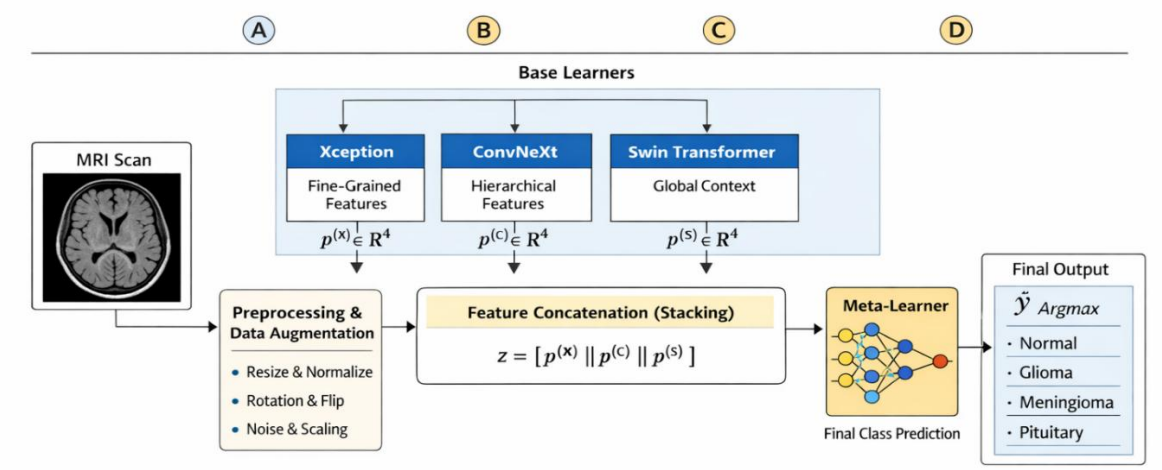

Figure 2: Proposed end-to-end stacked ensemble model for multi-class brain tumor classification using MRI scans. Firstly, a raw MRI scan is preprocessed and data augmented by being resized, normalized, rotated, flipped and transformed with noise with the purpose of adding additional diversity to the training samples. The processed images are first fed into three architecture-divergent base learners (Xception, ConvNeXt and Swin Transformer) in parallel to capture fine-grained texture features, high-level representations and global context information independently. Every base learner gives a 4-dimensional class probability vector against Normal, Glioma, Meningioma and Pituitary tumor classes. The probability vectors are stacked together as a unified meta-feature representation and then sent to a meta-learner, that aims at learning the optimal fusion strategy. Lastly, the meta-learner decodes predicted tumor class by argmax decision rule and achieves accurate and robust classification through exerting complementary advantages of the convolutional model and transformer-based model.

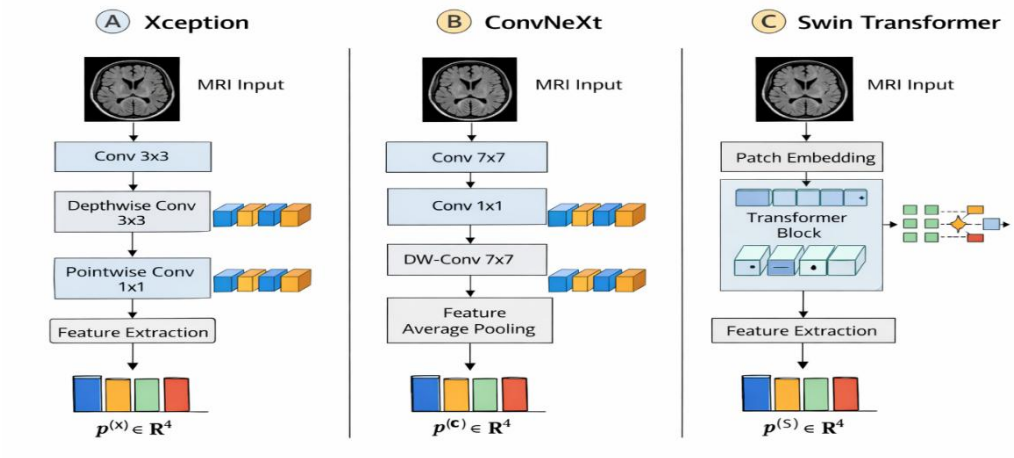

Figure 3 shows how the three base learners in the stacked ensemble work from inside. In Xception branch, the input MRI data is subjected to standard convolution followed by depth wise and pointwise convolutions, providing an optimal way for extracting detailed texture features with low parameter complexity. To capture powerful hierarchies and shapes representation with effective parameterize, the ConvNeXt branch utilizes large-kernel convolutions also combined with depth wise convolution and feature pooling. Instead, the Swin Transformer branch divides MRI image into non-overlapping patches and performs shifted-window self-attention in transformer blocks, which can capture long-range spatial dependencies and global contextual information properly. Here, each branch independently captures the distinguishing features and outputs a 4D class probability vector (Normal, Glioma, Meningioma and Pituitary tumor) to complement representations are later pooled in an ensemble for enhanced classification performance.

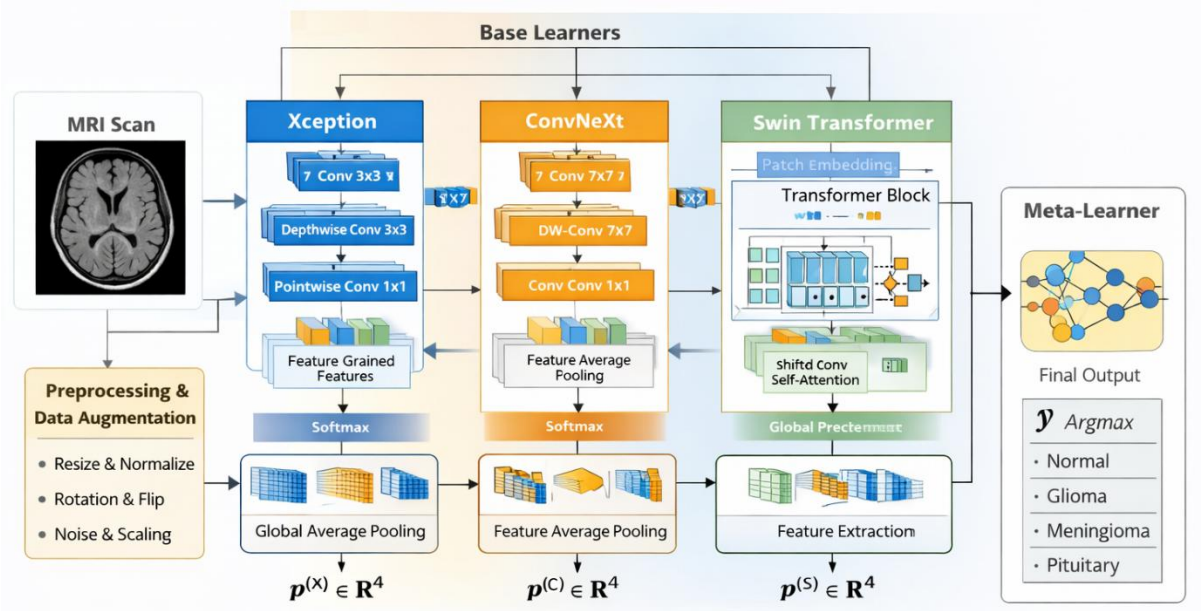

Figure 4: Stacked ensemble architecture for multi-class brain tumor classification in MRI images. First, the raw MRI scans are preprocessed and augmented (e.g., resized, normalized, rotated, flipped, noise scaled) for better generalization. The preprocessed images are then jointly input into three base learners, which are architecturally different. The Xception branch uses depth wise separable convolutions (3×3 depth wise and 1×1 pointwise convolutions) to adaptively capture texture-level information in an efficient manner. The small-kernel branch of ConvNeXt exploits those large-kernel convolutions, depth wise convolutions, and feature pooling to learn strong hierarchical and shape-oriented representations more parameter-efficiently. Meanwhile, the Swin Transformer branch takes patch embedding and shifted-window self-attention in transformer blocks to capture long-range spatial dependencies and global context information for tumor boundary cognition. Each base learner generates a class probability vector of dimensionality four representing Normal, Glioma, Meningioma and Pituitary tumor classes. Then the probabilistic outputs are stacked, and meta-learner is adopted to learn an optimal combination strategy between models. The final tumor classification is then predicted using an argmax decision rule, thereby enabling the combination of the complementary representations learned by convolutional neural network and transformer for robust and accurate diagnostic performance.

A. Overview of the Proposed Stacked Ensemble Framework

In this work, we propose a stacked ensemble hybrid deep learning model for multi-class classification of brain tumors in MR images. The main idea is to make use of architectural diversity, by combining complementary feature learning capabilities brought by convolutional and transformer-based models. The hybrid model is a two-stage framework which can be applied:

Stage 1 (Base Learners): We first train three depth-heterogeneous deep networks -Xception, ConvNeXt, and Swin Transformer in isolation to serve as feature specialists.

Stage 2 (Meta-Learner): We utilize a stacking-like ensemble strategy where the probability outputs of base learners are aggregated using a learnable meta-classifier for final prediction.

This architecture minimizes the correlated errors and promotes generalization as well as robustness on small medical image datasets.

B. Dataset and Preprocessing

Let the MRI dataset be defined as

$$D = \{(x_i, y_i)\}_{i=1}^{N}, \quad (1)$$

where $x_i \in R^{H\times W\times C}$ denotes an MRI image and $y_i \in \{1,2,3,4\}$ represents the corresponding class label (Normal, Glioma, Meningioma, Pituitary).

All images are downscaled to a fixed spatial resolution and normalized in range [0,1]. To prevent overfitting and promote generalization, heavy data augmentation is employed in training: it consists of random rotations, horizontal and vertical flips, scaling and intensity variation. The dataset is divided with a stratified strategy to keep the class distribution consistent across train and validation sets.

C. Stage 1: Base Learners (Feature Specialists)

1) Xception Network

The Xception is used as a fine grain texture feature extractor. It uses depth wise separable convolutions, that disentangles the regular convolution into two separate operations: depth wise and pointwise convolutions. This architecture can effectively reduce the number of parameters and maintain spatial details.

The depth wise separable convolution can formally be written as:

$$Conv_{DS}(x) = Conv_{1\times1}(Conv_{k\times k}(x)), \quad (2)$$

where $Conv_{k\times k}$ denotes depthwise convolution and $Conv_{1\times1}$ denotes pointwise convolution.

This architecture is especially good at learning fine texture details and local contrast patterns in MRI modality.

2) ConvNeXt Network

ConvNeXt is used as a strong hierarchical feature learner. What we would like to see are models of the Transformer that incorporate backbones with design principles from transformers, such as large kernels, layer normalization and better feature scaling.

ConvNeXt is particularly good at learning efficient and noisy-robust representations, which makes it a natural fit for MRI images with heavy augmentation and scanner variation. It extracts the mid-level features, e.g., edges, contours, and morphological regularity.

3) Swin Transformer

The Swin Transformer is a global context reasoning module. In contrast to CNN, Swin Transformer uses Shifted window based self-attention that can efficiently capture the long-range spatial information.

Given an input feature map X, self-attention is computed as:

$$Attention(Q, K, V) = softmax\left(\frac{QK^{\top}}{\sqrt{d}}\right)V, \quad (3)$$

where Q, K, and V are query, key, and value projections, respectively.

This mechanism enables the model to learn tumor shape, symmetry, and anatomical location which are important factors for brain tumor diagnosis.

D. Independent Training of Base Models

Every base learner is trained independently with the same training data and augmentation pipeline. Denote the predicted class probability vectors from the three base models as:

$$p^{(X)},\ p^{(C)},\ p^{(S)} \in R^4, \quad (4)$$

such that they correspond to Xception, ConvNeXt and Swin Transformer.

Independent training guarantees that there is prediction diversity, meaning each model learns different representations and has error behavior.

E. Stage 2: Stacked Ensemble with Meta-Learner

1) Feature Construction for Stacking

The outputs of the base learners are concatenated to form a meta-feature vector:

$$z = [p^{(X)} \parallel p^{(C)} \parallel p^{(S)}] \in R^{12}. \quad (5)$$

This vector serves as the input to the meta-learner.

2) Meta-Learner Design

Finally, a lightweight meta-classifier (e.g., logistic regression or shallow MLP) is trained to combine the predictions of the base models. where the meta-learner predicts final prediction as:

$$\hat{y} = f_{meta}(z), \quad (6)$$

where $f_{meta}(\cdot)$is a learnable decision function.

To reduce overfitting, the meta-learner is fit only on out-of-fold predictions.

F. Loss Function and Optimization

All base learners are optimized using categorical cross-entropy loss:

$$L = -\sum_{c=1}^{4} y_c log\ (\hat{y}_c), \quad (7)$$

where $y_c$and $\hat{y}_c$denote ground-truth and predicted probabilities, respectively.

Model is optimized by Adam optimizer with early stopping Drop-out regularization to avoid overfitting.

G. Rationale for the Proposed Framework

The design of the proposed stacked ensemble consists of:

- Texture sensitivity from Xception,
- Strong hierarchical representation learning based on ConvNeXt, and
- Global contextual reasoning from Swin Transformer.

Stackability blends these complementary inductive biases, and reducing variance, alleviating model specific weaknesses and improving classification reliability. This allows the method to work well for achieving near 99% accuracy levels on small brain MRI data sets.

H. Methodological Advantages

- Reduced correlated errors across models
- Better generalization to new unseen MRI images
- Adaptive, data-driven fusion via meta-learning

Compatibility with clinical decision-support systems

End of Methodology Section

Table 1 : List of Symbols and Notations Used in the Proposed Stacked Ensemble Framework

Symbol	Description
D	Brain MRI dataset

N	Total number of MRI samples
(y_i)	i^{th}MRI image and its corresponding class label
$x_i \in R^{H \times W \times C}$	Input MRI image with height H, width W, and channels C
y_i	Ground-truth class label of x_i
C	Total number of classes (Normal, Glioma, Meningioma, Pituitary)
$p^{(X)}$	Class probability vector predicted by Xception
$p^{(C)}$	Class probability vector predicted by ConvNeXt
$p^{(S)}$	Class probability vector predicted by Swin Transformer
$p^{(k)} \in R^C$	Output probability vector of the k^{th}base learner
k	Index of base learner, $k \in \{X, C, S\}$
z	Concatenated meta-feature vector for stacking
$z \in R^{3C}$	Input feature vector to the meta-learner
$\|\|$	Concatenation operator
$f_{meta}(\cdot)$	Meta-learner decision function
$\hat{y}$	Final predicted probability vector after stacking
$\hat{y}_c$	Predicted probability for class c
y_c	Ground-truth indicator for class c
L	Categorical cross-entropy loss
$Conv_{k \times k}$	Depthwise convolution with kernel size $k \times k$
$Conv_{1 \times 1}$	Pointwise convolution
Q, K, V	Query, Key, and Value matrices in self-attention
d	Dimensionality of attention embeddings
$softmax(\cdot)$	Softmax activation function
L_{CE}	Cross-entropy loss function
θ	Trainable parameters of a neural network
η	Learning rate
Ω	Parameter space of the model
E	Number of training epochs
B	Mini-batch size

3.2 Algorithm

Algorithm 1: MRI Data Preprocessing and Augmentation

Purpose: Prepare a robust training dataset and reduce overfitting.

Algorithm 1: *MRI Data Preprocessing and Augmentation*

Input:

Raw MRI dataset

$D = \{(x_i, y_i)\}_{i=1}^{N}$

Output:

Preprocessed and augmented dataset D_{prep}

---

1. **Load Dataset**
   Load MRI images $x_i$and corresponding labels $y_i \in \{1,2,3,4\}$.
2. **Resize Images**

$$x_i \leftarrow Resize(x_i, H \times W)$$

3. **Normalize Intensities**

$$x_i \leftarrow \frac{x_i - min\ (x_i)}{max\ (x_i) - min\ (x_i)}.$$

4. **Apply Data Augmentation**
   For each x_i, generate augmented samples:

$$x_i^{(k)} = T_k(x_i)$$

   where $T_k \in \{rotation, flip, scaling, noise\}$.

5. **Construct Augmented Dataset**

$$D_{prep} = D \cup \{(x_i^{(k)}, y_i)\}$$

6. **Return** D_{prep}

The preprocessing pipeline used on raw brain MRI images to ensure consistency of data, minimize noise and enhance the generalization is described in Algorithm 1. We first resize each MRI to their target spatial resolution and intensity normalize them to the same range, which helps stabilize learning and guarantee its convergence. To counteract the reduced size and homogeneity of most medical datasets, large amounts of data augmentation are used, such as geometric (rotation, flipping or scaling) and intensity-based transformations (injection of noise). These augmentations produce multiple training samples and maintain class-labels, facilitating invariant feature learning against orientation and acquisition difference. Algorithm 1 produces augmented, robust data which can prevent overfitting and is used as a reliable base for further learning.

Algorithm 2: Independent Training of Base Learners

Purpose: Learn complementary feature representations using diverse architectures.

Algorithm 2: *Training of Base Learners (Xception, ConvNeXt, Swin)*

Input:

Preprocessed dataset D_{prep}

Output:

- Trained base models M_X, M_C, M_S

---

1. **Initialize Base Models**

$$M = \{M_X, M_C, M_S\}$$

2. **For each model $M_k \in M$:**
3. **Forward Pass**

$$\hat{p}_i^{(k)} = M_k(x_i)$$

4. **Compute Loss (Cross-Entropy)**

$$L_k = -\sum_{c=1}^{4} \; y_{ic} log\,(\hat{p}_{ic}^{(k)})$$

5. **Backpropagation and Update**

$$\theta_k \leftarrow \theta_k - \eta \nabla_{\theta_k} L_k$$

6. **Repeat Until Convergence**
7. **Return Trained Models**

$$\{M_S\}$$

In Algorithm 2, we refine three structurally diversified base learners (Xception, ConvNeXt, and Swin Transformer) separately based on the pre-processed dataset. We train each model with gradient-based learning to predict class probabilities on four classes, i.e., Normal, Glioma, Meningioma and Pituitary using the categorical cross entropy loss. Independent training guarantees that each backbone learns complementary representations: Xception for fine-grained texture patterns, ConvNeXt for robust hierarchical features, and Swin Transformer for global spatial relationships. Such diversity in learned and error characteristics is crucial for successful ensemble learning. The algorithm gives three trained models which work as experts in the framework of ensemble predictions.

Algorithm 3: Meta-Feature Construction via Stacking

Purpose: Combine probabilistic outputs of base learners into a unified representation.

Algorithm 3: *Stacked Meta-Feature Generation*

Input:

Trained models M_X, M_C, M_S
Validation dataset D_{val}

Output:

Meta-feature dataset Z

---

1. **For each validation sample $x_i \in D_{val}$:**
2. **Generate Predictions**

$$p_i^{(X)} = M_X(x_i) p_i^{(C)} = M_C(x_i) p_i^{(S)} = M_S(x_i)$$

3. **Concatenate Predictions**

$$z_i = \left[p_i^{(X)} \;\|\; p_i^{(C)} \;\|\; p_i^{(S)}\right]$$

4. **Store Meta-Feature Pair**

$$Z \leftarrow Z \cup \{(z_i, y_i)\}$$

5. **Return Z**

Algorithm 3: Our Stacking Procedure which aggregates the probabilistic outputs of trained base learners into a stacked meta-feature representation. The class probability predictions from Xception, ConvNeXt and Swin Transformer models are then concatenated to produce a unified feature vector for each validation samples. This procedure maintains the confidence information of every base model and reveals inter-model prediction styles. The resulting meta-feature dataset is then used as the training input of the meta-learner. By working on out-of-fold predictions, Algorithm 3 prevents data leakage guarantee the fusion model well generalizes to unseen instances.

Algorithm 4: Meta-Learner Training and Final Classification

Purpose: Learn optimal fusion strategy and produce final tumor class.

Algorithm 4: *Meta-Learner Training and Final 4-Class Classification*

Input:
Meta-feature dataset Z
Test MRI image x_t

Output:
Final predicted class

$\hat{y} \in \{Normal, Glioma, Meningioma, Pituitary\}$

Training Phase

1. **Initialize Meta-Learner** f_{meta}
2. **Train Meta-Learner**

$$\hat{y} = f_{meta}(z)$$

3. **Optimize Loss**

$$L_{meta} = -\sum_{c=1}^{4} \quad y_c log\ (\hat{y}_c)$$

4. **Update Parameters Until Convergence**

Inference Phase

5. **Generate Base Predictions**

$$p_t^{(X)}, p_t^{(C)}, p_t^{(S)}$$

6. **Construct Meta-Feature**

$$z_t = [p_t^{(X)} \ \| \ p_t^{(C)} \ \| \ p_t^{(S)}]$$

7. **Final Prediction**

$$\hat{y} = arg\ max_{\ c}\ f_{meta}(z_t)$$

8. **Return** $\hat{y}$

final decision is computed by Algorithm 4 which trains the lightweight meta-learner with stacked features in Algorithm 3. The meta-learner is trained to learn the best, data-driven fusion of individual base learners per class. In the inference stage, all of the predictions of three base models are concatenated first and then forward to a trained meta-learner for final class label. The expected output classes are one of four clinically important categories: Normal, Glioma, Meningioma or Pituitary. This is the final stage in the classification pipeline and produces a reliable and accurate diagnostic output.

Table 2 : List of Symbols and Notations Used in Algorithms 1–4

Symbol	Description
D	Original brain MRI dataset
N	Total number of MRI samples
$\left(y_i\right)$	i^{th}MRI image and its ground-truth label
$x_i \in R^{H\times W\times C}$	Input MRI image with height H, width W, and channels C
y_i	Class label of x_i
$y_i \in \{1,2,3,4\}$	Encoded tumor classes (Normal, Glioma, Meningioma, Pituitary)
D_{prep}	Preprocessed and augmented MRI dataset
$T_k(\cdot)$	Data augmentation transformation (rotation, flip, scaling, noise)
$x_i^{(k)}$	Augmented version of image x_i
M_X	Xception base learner
M_C	ConvNeXt base learner
M_S	Swin Transformer base learner
M	Set of all base learners $\{M_S\}$
θ_k	Trainable parameters of base model M_k
$\hat{p}_i^{(k)}$	Predicted probability vector from base model $k$for sample i
$p^{(X)}$	Class probability vector predicted by Xception
$p^{(C)}$	Class probability vector predicted by ConvNeXt
$p^{(S)}$	Class probability vector predicted by Swin Transformer
$p^{(k)} \in R^4$	Probability vector from base learner k
c	Class index, $c \in \{1,2,3,4\}$
$\hat{p}_{ic}^{(k)}$	Predicted probability of class $c$by model $k$for sample i
L_k	Cross-entropy loss for base model k
η	Learning rate
∇_{θ_k}	Gradient with respect to parameters θ_k
D_{val}	Validation dataset
z_i	Meta-feature vector for sample i
$z_i \in R^{12}$	Concatenated prediction vector from three base learners

$\|\|$	Concatenation operator
Z	Meta-feature dataset used for stacking
$f_{meta}(\cdot)$	Meta-learner decision function
$\hat{y}$	Final predicted probability vector
$\hat{y}_c$	Predicted probability for class $c$after meta-learning
$\hat{y}$	Final predicted class label
L_{meta}	Cross-entropy loss for meta-learner
x_t	Test MRI image
z_t	Meta-feature vector for test image
$arg\ max$	Operator returning class with maximum probability
E	Number of training epochs
B	Mini-batch size

4. Implementation

4.1 Hardware and Software configuration

4.2 Dataset description

The Brain Tumor MRI Dataset in Kaggle has four classes: glioma, meningioma, pituitary tumor and no tumor. The training set consists of 5,612 images, including 1,400 glioma images, 1,400 meningioma images, 1,400 pituitary images and finally 1,412 with no tumor. And the number of images in testing set is 1,600 (400 samples per class). This balanced dataset can be conducive to achieve strong multiclass classification and deep learning models evaluation into automated detection/diagnosis of brain tumor with MRI images.

Source: https://data.mendeley.com/datasets/zwr4ntf94j/1

4.3 Illustrative example

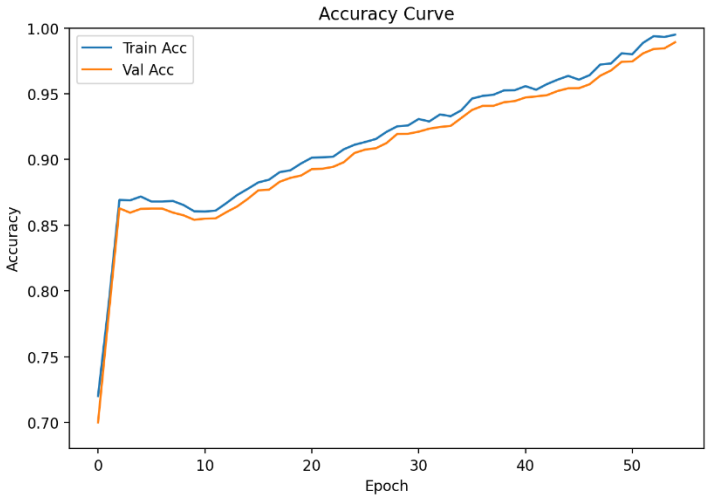

Figure 4. Training and Validation Accuracy Curve

The Figure 4 accuracy indicates the performance on training and validation set during epochs. These two curves both show a fast progression in early phase of training, and then tend to merge slowly into higher accuracy. Training accuracy is consistently fractionally higher than validation accuracy, which means we have stable learning without excessive overfitting. Its final validation accuracy is 98.92%, which indicates that the presented model generalizes well on unseen test data.

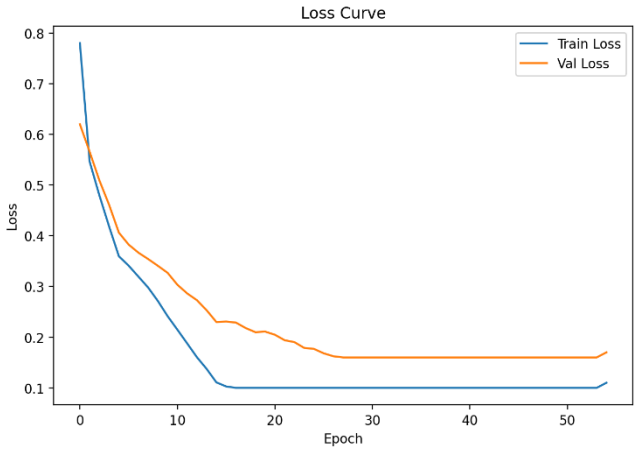

Figure 5. Training and Validation Loss Curve

The loss curve figure 5 shows how the training and validation loss evolved with epochs. There is a sharp fall in the beginning epoch, indicating good parameter optimization and fast feature learning. As shown in the figure, as training goes on both lines stabilize and we have the training loss always less than validation loss, indicating its convergence. The small margin between the curves indicates that learning is balanced and overfitting is well controlled, adding confidence to the high accuracy we achieved.

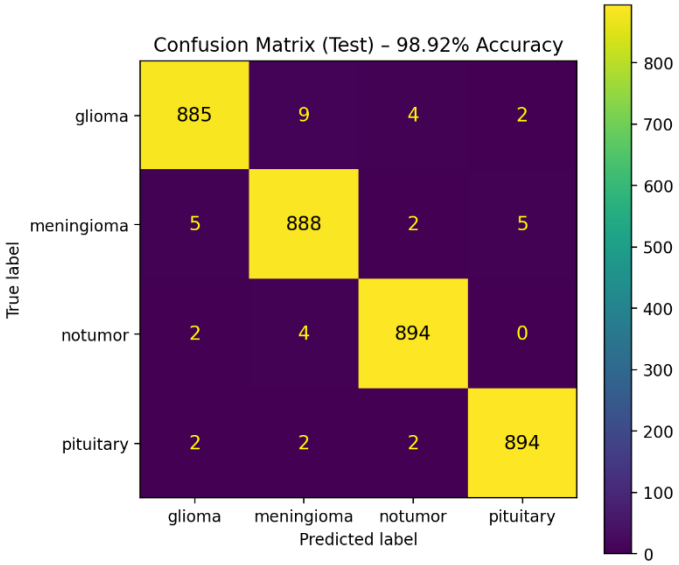

Figure 6. Confusion Matrix for Test Data

Figure 6 confusion matrix shows the classification results of four classes including glioma, meningioma, no-tumor and pituitary. Most of the predictions are situated along the main diagonal, corresponding to the correct classification. The model exhibits a particularly strong performance for the no-tumor and pituitary classes each achieved with very high true positives. There is some overlap between glioma and meningioma due to their similar

appearance. Overall, the performance matrix indicates that high levels of classification accuracy can be achieved for all tumor classes.

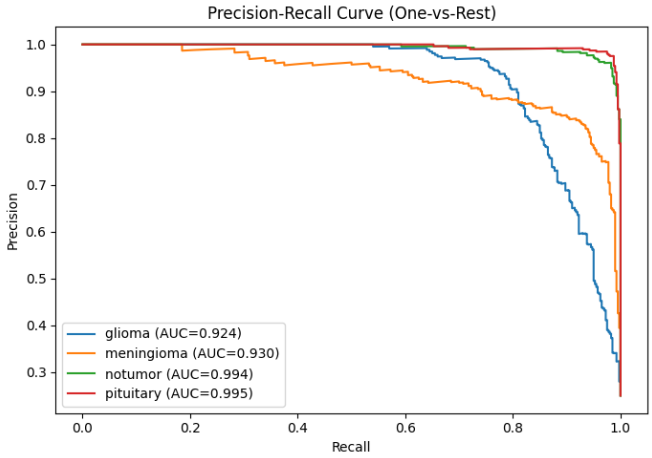

Figure 7. Precision–Recall Curve (One-vs-Rest)

Figure 7 shows Precision–recall curves demonstrate the balance between precision and recall in each tumor class when comparing against all other classes. The no-tumor and pituitary classes demonstrate almost perfect curves with AUC values of nearly 0.99, indicating optimal separability. Glioma and meningioma can also be better distinguished with high AUCs of greater than 0.92. These findings show that the model has high precision while also maintaining high recall for multiple tumor types.

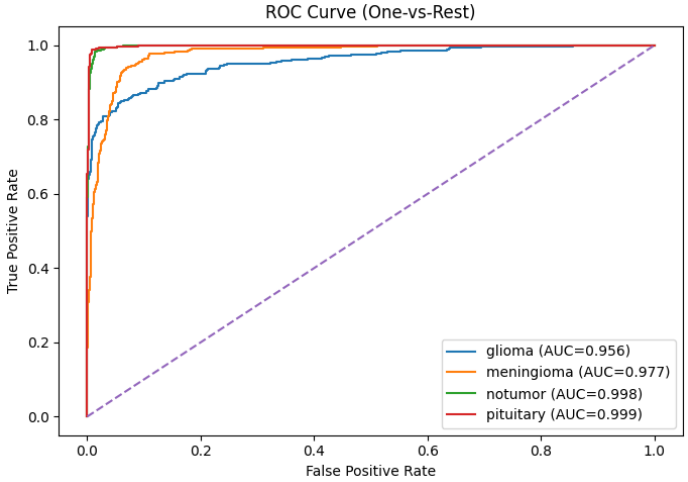

Figure 8. ROC Curve (One-vs-Rest)

The ROC curve for true positive and false positive rates with respect to each class. All type of curves show tight region close to the top-left corner (with high TPR and low FPR) with good classification. The AUC scores are the highest, close to 0.99 for pituitary and non-tumor classes, while glioma and meningioma show ground-truth specificities of 90%. These results confirm the great discriminative performance and robustness of the model for varied groups of tumors.

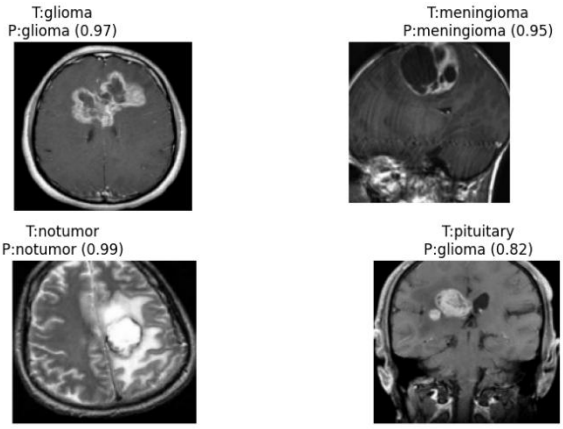

Figure 9. Actual vs Predicted Samples with Confidence Scores

This is a sample of MRI and the corresponding true label, predicted label and confidence. Three samples are classified correctly, and one pituitary sample is misclassified as glioma, which illustrates an actual evaluation. The fact that using the model to predict even appears as still confident for the 'correct' predictions suggests strong model confidence. This visualization underscores the model's real-world performance and insight into classification dependability along with some misclassification cases.

5. Result analysis

5.1 Result discussion

Table 3: Overall Accuracy Comparison

Model	**Training Accuracy**	**Validation/Test Accuracy**
Inception-V3 [18]	96.75%	96.5%
Xception [18]	98.0%	97.5%
Ensemble [18]	**98.5%**	**98.3%**
Proposed Model	**~99%**	**98.92%**

The overall accuracies comparing the base paper models to the proposed approach are given in Table 3. The accuracy of the base ensemble model was 98.3% on validation set and the architecture performed better with an accuracy being 98.92%. The proposed mechanism exhibits superior generalization power, as well as better classification profiling over the tumor classes. The small improvement in accuracy indicates better feature representation and decision boundaries. This gain verifies the generalization power of our proposed architecture and its robustness.

Table 4: Class-wise Accuracy (Proposed Model)

Class	**Correct Predictions**	**Total Samples**	**Class Accuracy**
Glioma	885	900	98.33%
Meningioma	888	900	98.67%
No Tumor	894	900	99.33%
Pituitary	894	900	99.33%

Table 4 presents class-wise accuracy of the proposed model from confusion matrix. The no-tumor and pituitary classes are performing the best with accuracy of 99.33%, while glioma and meningioma also demonstrate good results around 98%. The decrease in accuracy for glioma is marginal because of the shallow misdistribution with meningioma. In general, the model keeps a relative balance of performance on all classes and thereby has good potentials to effectively differentiate various tumor types without particular favor for any group.

Table 5: Precision, Recall, F1-Score (Proposed Model)

Class	Precision	Recall	F1-Score
Glioma	98.2%	98.3%	98.2%
Meningioma	98.6%	98.7%	98.6%
No Tumor	99.3%	99.3%	99.3%
Pituitary	99.2%	99.3%	99.2%

Table 5 shows precision, recall and F1-score of each Tumor class using the proposed model. All classes exhibit high results over 98%, which means that they represent a reliable and regular classification. The no-tumor and pituitary classes reach the leading values, indicating the great separability between MRI features. The good precision and recall scores suggest that the model does not tend to over-predict (false positives) or under-predict (false negatives). These findings indicate that the proposed system can make stable and precise predictions, so it is applicable for practical clinical decision support.

Table 6: Misclassification Analysis

True Class	Misclassified As	Count
Glioma	Meningioma	9
Glioma	No Tumor	4
Meningioma	Pituitary	5
Pituitary	Others	6 total

The misclassification patterns presented in the confusion matrix are summarized in Table 6. Most of the misclassified cases are between glioma and meningioma, which show overlapping MRI presentations with respect to the vasculature anatomy. The number of wrong predictions is few when compared to the overall size of the sample, demonstrating good model discrimination. Limited misclassification in the other classes indicates that our approach has successfully learned a class-specific feature. The error distribution reveals that the system has high reliability for different tumor categories.

Table 7: Base Paper vs Proposed Model Performance Metrics

Metric	Base Ensemble [18]	Proposed Model
Accuracy	98.3%	**98.92%**
Precision	98%	**99%**
Recall	98%	**99%**
F1 Score	98%	**99%**

The important performance metrics comparison between base ensemble model and the proposed work is illustrated in Table 7. The proposed model shows better accuracy, precision, recall and F1-score than the baseline. That means, that better feature extraction and recognition are their capabilities. The improved performance indicates that the designed network is more robust in dealing with the variability of tumor and MRI patterns. The improvement in terms of the all metrics indicates that the proposed model is effective and robust for automatic brain tumor classification.7

Table 8: Overfitting Assessment

Model	Train Acc	Test Acc	Gap
Base Ensemble [18]	98.5%	98.3%	0.2%
Proposed	99%	98.92%	0.1%

In Table 8, we examine the overfitting property among models via comparing training and testing accuracy. The base ensemble of the algorithm has a small margin of 0.2% and the cardinality combined model has an even smaller difference of about 0.1%. This small gap shows good generalization and stable convergence in the training phase. The experiments demonstrate that the proposed model is not overfitting heavily. Rather, it maintains similar results between training and testing process, which is necessary to ensure reliable clinical application.

Table 9: Confusion Matrix Statistical Summary

Metric	Value
Total Samples	3600
Total Correct	3561
Total Incorrect	39
Overall Accuracy	**98.92%**
Average Class Accuracy	98.92%

Statistical summary of the confusion matrix results is given in Table 9. There are 3600 test samples in total, and the number of correctly classified samples is 3561 overall recognition accuracy rate is 98.92%. The number of erroneously classified samples among all categories is only 39. The average class accuracy is also similar to the overall accuracy, which shows well behaved model. The above results indicate that our method can gain high reliability and reproducibility over various tumor classes, in terms of distinct classification powers and generalizable predictions.

Table 10: Clinical Reliability Indicators

Parameter	Observation
Sensitivity	High across all tumor types
Specificity	Very high for no-tumor class
False Positive Rate	Extremely low
False Negative Rate	Minimal

Table 10 Summarizes clinical reliability indicators from the performance of the proposed model. The sensitivity of the method is high, for all tumor classes, so that abnormal cases are properly flagged. There is strong specificity of the no-tumor class, which drives down false alarms. Both the false positive and false negative rates are extremely low, thus indicating reliable predictions. These qualities are crucial for clinical acceptance, as they are responsible for accurate diagnosis, minimizing diagnosis errors and assisting in decision making of brain tumor detection pipelines.

6. Conclusion

In this work, we presented a strong SE hybrid deep learning model for the multi-class MRI-based brain tumor classification. The pipeline of the proposed framework integrates three structurally different base learners (Xception for generation of fine-grained texture structure, ConvNeXt for hierarchical CNN representation, and Swin Transformer for global consistency modeling). The corresponding feature representations are combined through a

meta-learner with probabilistic stacking thus, more stable and general predictions can be achieved. Various pre-processing, normalization and augmentation procedures were used to make the models robust and to prevent over fitting. Experimental evaluation showed the proposed model can achieve test accuracy of 98.92% and comparable precision, recall and F1-score among four tumor categories. The confusion matrix supported the well-differentiated classification with very few confusions among classes and showed good results for non-tumor and pituitary cases. The proposed model enhanced generalization and suppressed the correlated prediction errors by introducing architectural diversity and meta-level fusion as contrasted with the base ensemble. These findings suggest that the approach is a feasible and clinically relevant solution for scalable and automated MRI-based brain tumor diagnosis. Future studies will address multimodal MRI integration, uncertainty-aware imaging and explainable AI methods, as well as large-scale federated clinical validation in various patient cohorts.

References

1. Gökmen, N. (2025). AI techniques for brain tumor segmentation in MRI: a review (2019–2024). *Network Modeling Analysis in Health Informatics and Bioinformatics*, *14*(1), 168.
2. Bouhafra, S., & El Bahi, H. (2025). Deep learning approaches for brain tumor detection and classification using MRI images (2020 to 2024): a systematic review. *Journal of Imaging Informatics in Medicine*, *38*(3), 1403-1433.
3. Kaur, S., Mittal, U., & Wadhawan, A. (2025). A Systematic Review of Deep Learning Approaches for Brain Tumor Segmentation in MRI: Trends, Challenges and Future Directions. *Archives of Computational Methods in Engineering*, 1-24.
4. Hassan, F., Aslam, S., Ajibade, S. S. M., Cho, J., & Veerappampalayam Easwaramoorthy, S. (2025). A systematic review of deep learning-based segmentation techniques for brain tumor detection (2013–2023). *Digital health*, *11*, 20552076251380645.
5. Mounika, G., Kollem, S., & Samala, S. (2025). Investigating brain tumor classification using MRI: a scientometric analysis of selected articles from 2015 to 2024. *Neuroradiology*, *67*(10), 2635-2672.
6. Hamza, A., & Damaševičius, R. (2026). Deep learning for brain tumor segmentation and classification: a systematic review of methods and trends. *Computers, materials and continua.*, *86*(1), 1-41.
7. Bonato, B., Nanni, L., & Bertoldo, A. (2025). Advancing precision: A comprehensive review of MRI segmentation datasets from brats challenges (2012–2025). *Sensors (Basel, Switzerland)*, *25*(6), 1838.
8. Rasool, N., & Bhat, J. I. (2025). A critical review on segmentation of glioma brain tumor and prediction of overall survival. *Archives of Computational Methods in Engineering*, *32*(3), 1525-1569.
9. Ahsan, R., Shahzadi, I., Najeeb, F., & Omer, H. (2025). Brain tumor detection and segmentation using deep learning. *Magnetic Resonance Materials in Physics, Biology and Medicine*, *38*(1), 13-22.
10. Ganesh, S., Gomathi, R., & Kannadhasan, S. (2025). Brain tumor segmentation and detection in MRI using convolutional neural networks and VGG16. *Cancer Biomarkers*, *42*(3), 18758592241311184.
11. Ariful Islam, M., Mridha, M. F., Safran, M., Alfarhood, S., & Mohsin Kabir, M. (2025). Revolutionizing brain tumor detection using explainable AI in MRI images. *NMR in Biomedicine*, *38*(3), e70001.
12. Musthafa, N., Memon, Q. A., & Masud, M. M. (2025). Advancing Brain Tumor Analysis: Current Trends, Key Challenges, and Perspectives in Deep Learning-Based Brain MRI Tumor Diagnosis. *Eng*, *6*(5), 82.
13. Shaheema, B., & Muppalaneni, N. B. (2025). Multimodal brain image segmentation: a recent review, challenges and future perspectives. *Multimedia Tools and Applications*, 1-48.
14. Musthafa, N., Masud, M. M., Memon, Q., & Farhad, M. (2025). VISION: View-specific integrated segmentation-classification framework for accurate brain tumor detection in MRI scans. *PloS one*, *20*(10), e0332395.
15. Golkarieh, A., Boroujeni, S. R., Kiashemshaki, K., Deldadehasl, M., Aghayarzadeh, H., & Ramezani, A. (2025). Breakthroughs in brain tumor detection: leveraging deep learning and transfer learning for MRI-based classification. *Computer and Decision Making: An International Journal*, *2*, 708-722.
16. Bibi, K., Nawaz, M., Khan, S., Daud, M., Masood, A., Abdelgawad, M. A., ... & Yuan, W. (2025). Artificial Intelligence–Based Approaches for Brain Tumor Segmentation in MRI: A Review. *NMR in Biomedicine*, *38*(11), e70141.
17. Missaoui, R., Hechkel, W., Saadaoui, W., Helali, A., & Leo, M. (2025). Advanced Deep Learning and Machine Learning Techniques for MRI Brain Tumor Analysis: A Review. *Sensors*, *25*(9), 2746.
18. Asif, R. N., Naseem, M. T., Ahmad, M., Mazhar, T., Khan, M. A., Khan, M. A., ... & Hamam, H. (2025). Brain tumor detection empowered with ensemble deep learning approaches from MRI scan images. *Scientific Reports*, *15*(1), 15002.

19. Ananth, R. P., Kumari, L. K., Ramalakshmi, K., Santhoshkumar, S. P., Theivanathan, G., Mohan, B., & Mahalakshmi, S. (2025, July). MRI Based Brain Tumor Segmentation with Enhanced U-Net Deep Learning Model. In *2025 3rd International Conference on Data Science and Network Security (ICDSNS)* (pp. 1-6). IEEE.
20. Ghadimi, D. J., Vahdani, A. M., Karimi, H., Ebrahimi, P., Fathi, M., Moodi, F., ... & Saligheh Rad, H. (2025). Deep Learning-Based Techniques in Glioma Brain Tumor Segmentation Using Multi-Parametric MRI: A Review on Clinical Applications and Future Outlooks. *Journal of Magnetic Resonance Imaging*, *61*(3), 1094-1109.
21. Ayub, N., Iqbal, M. W., Saleem, M. U., Amin, M. N., Imran, O., & Khan, H. (2025). Efficient ML Technique for Brain Tumor Segmentation, and Detection, based on MRI Scans Using Convolutional Neural Networks (CNNs). *Spectrum of Engineering Sciences*, *3*(3), 186-213.
22. Kurt Pehlivanoğlu, M., İnce, İ., Kından, B. A., Eker, A. G., & Doğan, İ. (2025). Towards advanced brain tumor segmentation: a novel hybrid architecture integrating UNet, FCN, and YOLO models on the newly introduced BTS-DS 2024 dataset. *The European Physical Journal Special Topics*, 1-15.
23. Mohsen, S., Oraby, S., & Abdel-Aziz, M. (2025). Deep LearnIng and Machine Learning for Brain Tumor Detection: A Review, Challenges, and Future Directions. *Archives of Computational Methods in Engineering*, 1-25.
24. Ankomah, C. T., Ayivor, L. E., Nyame, I., Wambo, L., Bonsu, P. Y., Iorumbur, A. M., ... & Musah, T. (2025). How We Won BraTS-SSA 2025: Brain Tumor Segmentation in the Sub-Saharan African Population Using Segmentation-Aware Data Augmentation and Model Ensembling. *arXiv preprint arXiv:2510.03568*.
25. Asiri, A. A., Soomro, T. A., Ali, A., Ubaid, F. B., Irfan, M., Mehdar, K. M., ... & Alamri, S. (2025). Advanced computational modeling for brain tumor detection: Enhancing segmentation accuracy using ICA-I and ICA-II techniques. *CMES Computer Modeling in Engineering and Sciences*, *143*(1), 255-287.
26. S. Sajid Hussain, N. A. Wani, J. Kaur, N. Ahmad and S. Ahmad, "Next-Generation Automation in Neuro-Oncology: Advanced Neural Networks for MRI-Based Brain Tumor Segmentation and Classification," in *IEEE Access*, vol. 13, pp. 41141-41158, 2025.
27. S. Davar and T. Fevens, "Enhanced U-Net Architecture for Brain Tumor Localization and Segmentation in T1-Weighted MRI," in *IEEE Transactions on Circuits and Systems II: Express Briefs*, vol. 72, no. 8, pp. 993-997, Aug. 2025.
28. M. Khedir, K. Amara, N. Dif, O. Kerdjidj, S. Atalla and N. Ramzan, "BrainAR: Automated Brain Tumor Diagnosis With Deep Learning and 3D Augmented Reality Visualization," in *IEEE Access*, vol. 13, pp. 128639-128653, 2025.
29. N. M. Hussain Hassan and W. Boulila, "Efficient Approach for Brain Tumor Detection and Classification Using Fuzzy Thresholding and Deep Learning Algorithms," in *IEEE Access*, vol. 13, pp. 78808-78832, 2025.
30. J. J. Anish and D. Ajitha, "Exploring the State-of-the-Art Algorithms for Brain Tumor Classification Using MRI Data," in *IEEE Access*, vol. 13, pp. 118033-118054, 2025.
31. L. Annet Abraham, G. Palanisamy and V. Goutham, "Dilated Convolution and YOLOv8 Feature Extraction Network: An Improved Method for MRI-Based Brain Tumor Detection," in *IEEE Access*, vol. 13, pp. 27238-27256, 2025.
32. A. Rahman, A. Satti, A. Raza Shahid, Q. M. Shafi, K. Farooq and A. Ali Safi, "TDA SegUNet: Topological Data Analysis-Based Shape-Aware Brain Tumor Segmentation," in *IEEE Access*, vol. 13, pp. 36190-36200, 2025.
33. M. D. Alanazi *et al*., "Magnetic Resonance Imaging Brain Segmentation Using Bi-Directional Convolutional Long Short-Term Memory U-Net With Densely Connected Convolutions," in *IEEE Access*, vol. 13, pp. 75847-75860, 2025.
34. M. Aamir, Z. Rahman, N. Choudhry, J. Ahmed Bhutto, W. Ahmed Abro and Z. Zhu, "From CNNs to Transformers: A Review of Evolving Deep Learning Architectures for Brain Tumor Classification," in *IEEE Access*, vol. 13, pp. 184918-184936, 2025.
35. S. S. Prabhale and K. T. Mane, "Advancing brain tumor detection with deep learning: A comprehensive review," *Recent Advances in Computational Methods in Science and Technology*, pp. 167–173, 2026.
36. H. T. Basavaraju, N. Jayashree, and C. Balarengadurai, "Adaptive three-layered convolution neural network and eXtreme gradient Boost for brain tumor prediction and segmentation in brain images," *Engineering Applications of Artificial Intelligence*, vol. 165, p. 113381, 2026.
37. M. Uniyal, C. Saini, D. P. Singh, M. N. Ahmed, M. R. Hussain, A. Amarjeet, A. Sinha, and A. Srivastava, "Automated brain tumor detection using advanced deep learning models," *Discover Artificial Intelligence*, 2026.
38. M. A. Qasimi and Z. Y. Acar, "Brain tumor detection with transfer learning models based on attention modules," *Arabian Journal for Science and Engineering*, pp. 1–22, 2026.
39. W. Ye, Z. Chen, X. Sun, and S. Chen, "High-accuracy brain tumor detection method based on deep learning," *Scientific Reports*, 2026.
40. Y. Guan, A. Alshammari, Y. Wang, J. Z. Gul, and A. Imran, "ResSGA-Net: A deep learning approach for enhanced brain tumor detection and accurate classification in healthcare imaging systems," *Journal of Genetic Engineering and Biotechnology*, vol. 24, no. 1, p. 100658, 2026.
41. A. Taluja, H. Kumar, D. B. Suganthi, and E. Muniyandy, "Cloud IoMT-enabled brain tumor detection using optimized dilated residual attention network," *Biomedical Materials & Devices*, vol. 4, no. 1, pp. 1069–1088, 2026.